Compressive properties of the unidirectionally solidified Sb-Ge eutectic

M. SAHOO, D. BARAGAR, R. W. SMITH

Department of Metallurgical Engineering, Queen's University, Kingston, Ontario, Canada K7L 3N6

The structure and compressive properties of the faceted/faceted Sb—Ge eutectic, unidirectionally solidified over a wide range of growth rates, have been examined and compared with those of the faceted/non-faceted Al—Si and Zn—Ge eutectics. The UCS of the Sb—Ge eutectic was found to be independent of the scale of the microstructure. It is considered that this behaviour is the result of the presence of a brittle matrix and poor matrix/second phase coherence.

1. Introduction

From the standpoint of morphological characterization, binary eutectics can be classified into two broad fields: regular or non-faceted/non-faceted (n.f./n.f.) eutectics and anomalous or faceted/non-faceted (f./n.f.) eutectics [1–4]. The characterizing parameter used for such classification are the entropy of solution ($\Delta S\alpha$) and volume fraction (V_f) of the minor constituents and the growth conditions. It is now established that when ΔS for the minor constituent exceeds some critical value (5.5 cal K^{-1} mol^{-1}), the phase tends to facet. The authors have shown that the morphology of the faceted phase is markedly dependent on the V_f, growth rate and temperature gradient at the solid/liquid interface [2] and hence the f./n.f. eutectics may be placed in one of the four sub-groups, namely broken-lamellar, irregular, complex-regular and quasi-regular (in ascending order of the volume fraction of the faceting phase). The group of anomalous eutectics in which $V_f = 6$ to 18% has been classified as "irregular" and many common industrial alloys are in this group; e.g., Al—Si and Fe—C. In an attempt to characterize the mechanical properties of eutectics, we have examined the tensile and compressive properties of a number of unidirectionally solidified regular and anomalous eutectics where V_f varied between 6 and 18% [5–9].

To date there is very little information on the eutectic morphology and mechanical properties of a faceted/faceted (f./f.) eutectic. As part of a continuing programme to characterize the structure and mechanical properties of binary eutectics, we chose to investigate the relationship between the microstructure and mechanical properties of a f./f. eutectic whose V_f was between 6 and 18%. An examination of the phase diagrams [10–12] and our previous eutectic classification scheme [2] showed that the Sb—Ge eutectic system can be taken as a typical example of an irregular f./f. eutectic. It has 12% by volume of the faceted Ge phase in the faceted rhombohedral Sb matrix. In addition, the Sb—Ge eutectic is another example of the metal/non-metal combinations. Thus its structure and mechanical properties following unidirectional solidification over a wide range of growth conditions can be compared with those of Al—Si [5] and Zn—Ge [7] eutectic alloys with a view to examining the influence of the matrix constraints during deformation.

2. Experimental

The Sb—Ge eutectic alloy containing 11 wt % Ge was prepared from 99.999% pure elemental materials. Weighed amounts of Sb—Ge were melted in an atmosphere of argon in a 30 mm vycor tube and shaken vigorously to encourage complete mixing. The molten alloy was sucked into 5 mm i.d. pyrex tubes. The solidified rods

were sealed into argon-filled 6 mm i.d. vycor tubes and directionally solidified by lowering into a water-jacket.

The experimental procedures for compression testing and metallographic examination were similar to those mentioned in [8] except that the etching solution consisted of equal parts of concentrated nitric acid, acetic acid and water. A Phillips AMR 900 Scanning Electron Microscope (SEM) was used to examine the as-grown microstructure.

3. Results
3.1. Eutectic morphology
Representative optical micrographs of transverse sections through Sb$-$11 wt % Ge eutectic alloys directionally solidified at various growth rates are shown in Figs. 1a to f. Optical micrographs of longitudinal sections corresponding to some of these transverse sections are shown in Figs. 2a and b.

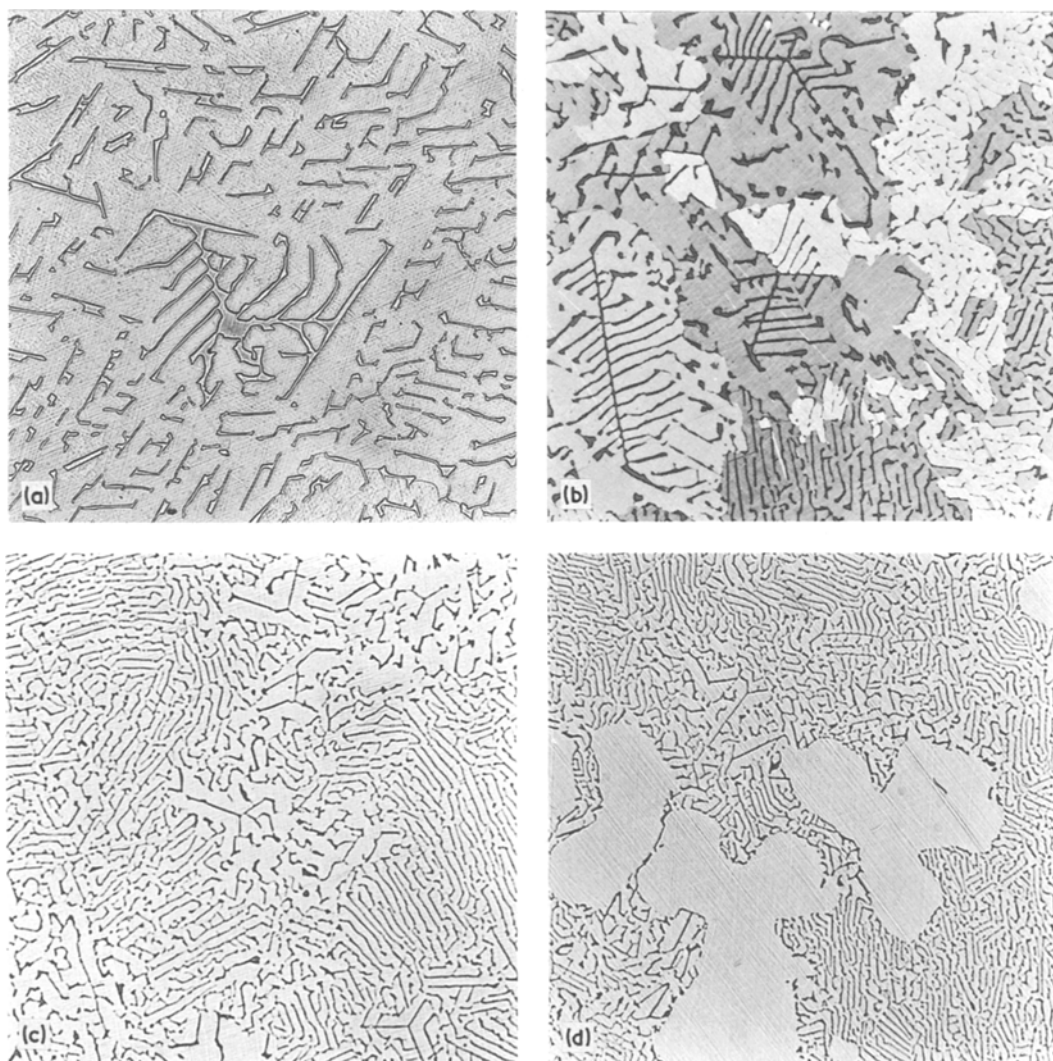It is evident that in Sb$-$Ge eutectic alloys directionally solidified at very low growth rates

Figure 1 Optical micrographs of transverse sections through directionally solidified Sb$-$Ge eutectic alloys showing the Ge morphology at various growth rates. (a) $R = 2.5$ mm h^{-1}, ($\times 96$); (b) $R = 5.4$ mm h^{-1}, polarized light, ($\times 96$); (c) $R = 42$ mm h^{-1}, ($\times 192$); (d) $R = 108$ mm h^{-1}, ($\times 240$); (e) $R = 170$ mm h^{-1}, ($\times 96$); (f) $R = 1330$ mm h^{-1}, ($\times 96$).
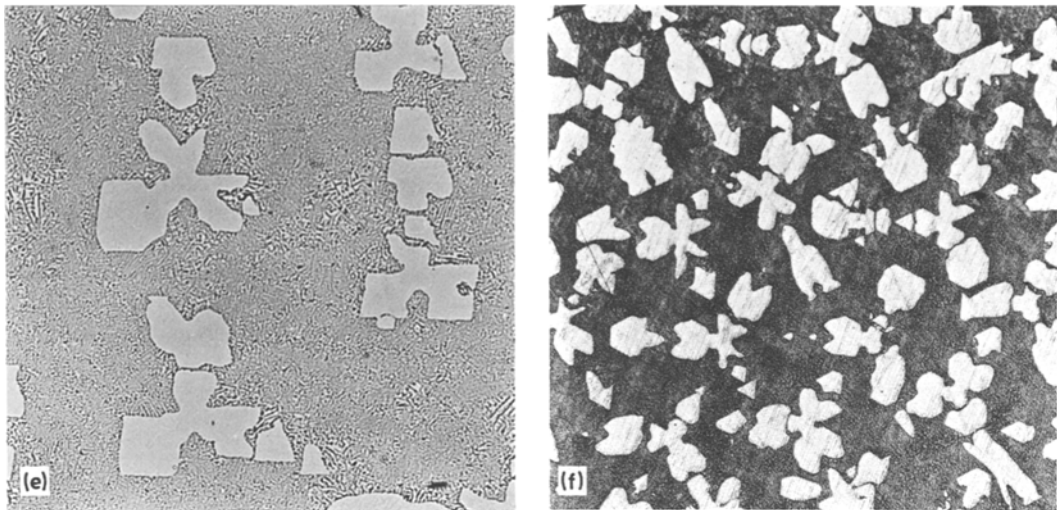
Figure 1 continued.

(2.5 and 5.4 mm h⁻¹), the Ge dendrites grew parallel to the growth direction. However, very little branching of these dendrites was observed. As a result the branched dendritic form of Si and Ge observed in the transverse section of Al–Si and Zn–Ge eutectic alloys respectively [5, 7] was not found to be present in abundance. Instead, Ge platelets were found to grow parallel to each other in some areas. Similar observations were made by Kerr and Winegard [13]. Fig. 2a, which is the longitudinal section of the quenched growth front corresponding to Fig. 1b, shows that, in common with the observations made in the metal/non-metal eutectic alloys, the growth front is non-isothermal.

As the growth rate was increased, the Ge platelets became finer and more aligned with each other. In addition, branched plates and some complex-regular cells were also observed in the transverse sections. At a growth rate of 108 mm h⁻¹, the faceted Sb primaries started to appear. It is observed from Fig. 2b, which is the longitudinal section corresponding to Fig. 1d, that the angle between the Sb facets is about 87.5° which is also the angle between the ⟨1 0 0⟩ axes of the rhombohedral unit cells. This indicates
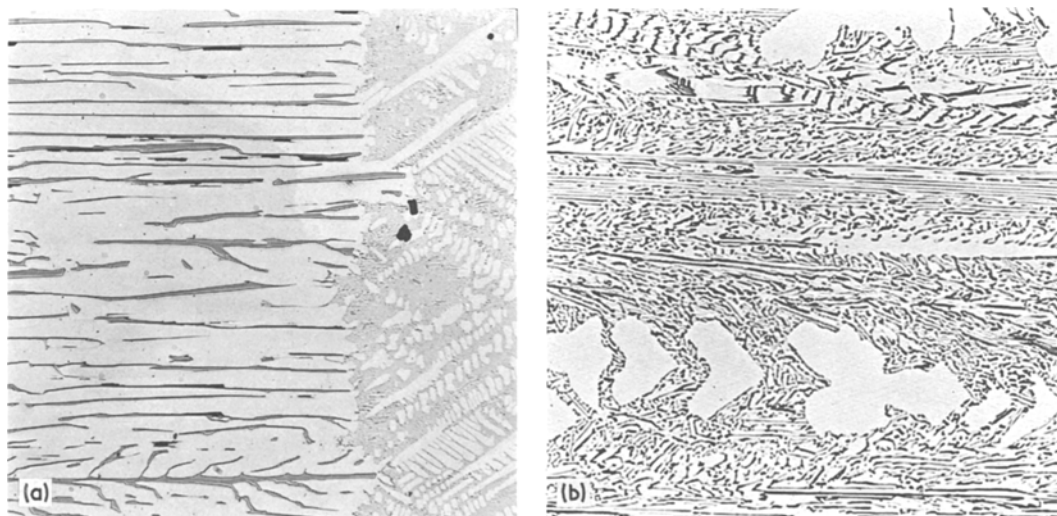

Figure 2 Optical micrographs of longitudinal sections corresponding to Figs. 1b and d respectively. (a) $R = 5.4$ mm h⁻¹, (× 96), quenched growth front; (b) $R = 108$ mm h⁻¹, (× 115).
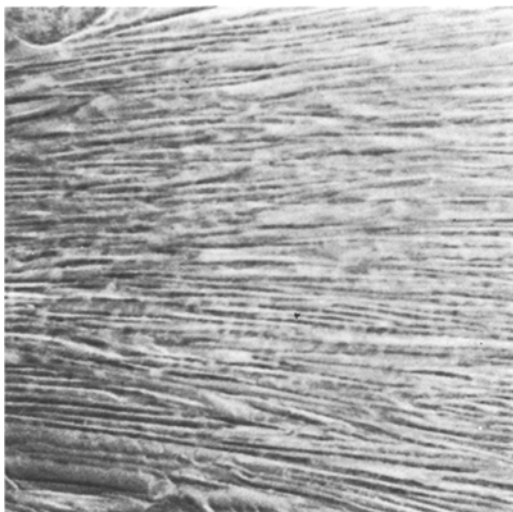
Figure 3 Scanning electron micrograph of Sb–Ge eutectic alloy directionally solidified at 4000 mm h^{-1} (× 1920).

that the Sb primaries grow in the ⟨1 1 0⟩ direction.

At a growth rate of 1330 mm h^{-1} a modified microstructure was produced, Fig. 1f. As in the Al–Si and Zn–Ge system, modification results in the presence of Sb primaries surrounded by eutectic microstructure in which the faceted Ge phase has become fibrous in nature. A comparison of this micrograph with that produced at a growth rate of 170 (Fig. 1e) and 4000 (Fig. 8b) mm h^{-1} reveal that there is a substantial increase in the volume fraction of the Sb primaries with growth rate. A scanning electron micrograph of the

heavily etched longitudinal section (Fig. 3) of the growth modified Sb–Ge eutectic suggests that the fibres run parallel to the growth direction. It is interesting to note that the primary dendrites seen in Fig. 1 become less angular as the growth rate increases. This is presumably the result of an increase in the undercooling in the system.

In order to determine the fineness of the microstructure caused by increasing growth rates, the linear-intercept method was used to measure the interparticle spacing (λ) in transverse sections. These data are summarized in Fig. 4. In this plot each point is the average of at least 10 readings. It should be noted that for specimens containing Sb primaries the λ measurements were carried out in areas containing Sb dendrite-free eutectic structures. From Fig. 4 the interparticle spacing measurements are found to correspond to a relationship

$$\lambda = AR^{-1/2} \qquad (1)$$

These unidirectionally solidified specimens were found to be polycrystalline. The grain size, observed under polarized light, Fig. 1b, was found to be large compared to the particle size and spacing.

Metal/non-metal eutectic combinations containing either Si or Ge as the minor faceting constituent are usually modified by the addition of very small amounts of sodium (<0.02%). In the case of the Sb–Ge eutectic both phases are faceting and thus it was of interest to see the effect of Na on its microstructure. With a fine thermocouple placed in an open pot, no under-
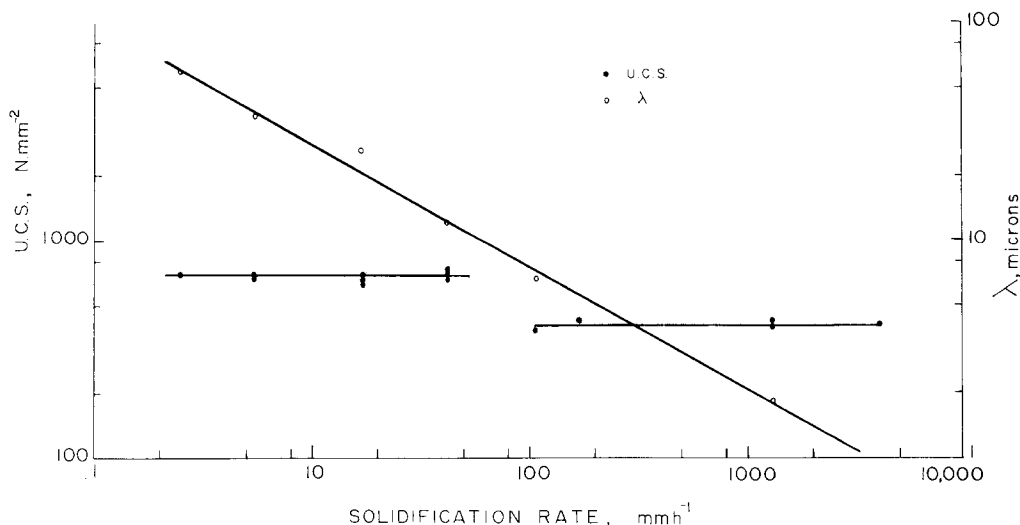

Figure 4 Effect of solidification rate on the interparticle spacing and the UCS.

1568

TABLE I Undercooling measured in Sb–Ge eutectic alloys

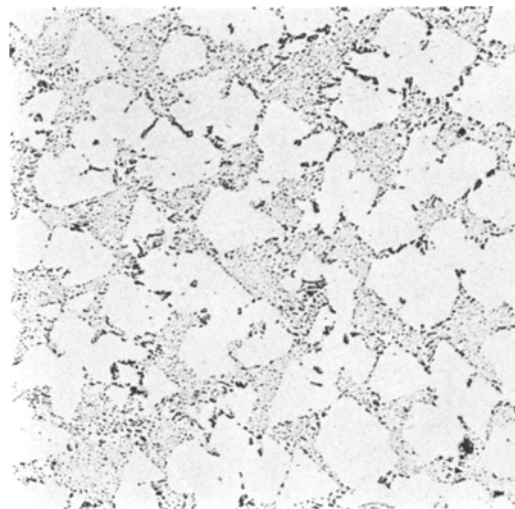| Modifying element	(wt %)	Undercooling (°C)
Na	0.08	0
	0.30	3.7
	0.40	5.0
	0.45	6.0
	0.53	6.0
	0.80	9.5
Cs	0.3	14.0

Figure 6 Optical micrograph of the caesium-modified Sb–Ge eutectic directionally solidified at 18 mm h^{-1}. 0.3 wt % (0.2 at %) caesium added (× 96).

cooling was observed with the addition of 0.08 wt % Na and the microstructure was found to remain unmodified. With increasing amounts of Na, there was an increase in the measured undercooling (Table I) and the microstructure started to be modified. Fig. 5 is a typical optical micrograph of the Na-modified (0.8 wt % Na or 4 at % Na) Sb–Ge eutectic directionally solidified at a rate of 18 mm h^{-1}. This microstructure depicts faceted Sb primaries surrounded by a slightly modified eutectic microstructure. The fineness of microstructure was found to vary from area to area. In some areas large chunks of faceted Ge particles were also observed.

In the case of the modified Al–Si eutectic, the non-faceted aluminium primaries grow ahead of the eutectic and, it is presumed, the faceted silicon phase grows in a coupled manner with the eutectic aluminium phase when the undercooling

Figure 5 Optical micrograph of the sodium-modified Sb–Ge eutectic directionally solidified at 18 mm h^{-1}. 0.8 wt % (4 at %) sodium added (× 96).

required for the growth of the two phases becomes equal. By analogy, the presence of the Sb primaries in the Sb–Ge eutectic indicates that the faceted Sb primaries also grow faster than the eutectic. However, sufficient undercooling is not produced for the coupled growth of the Sb and Ge phases. As a result, an entirely fibrous morphology is not obtained.

It has been observed that chemisorption of alkali metals on Bi increases in the series Na < K < Rb < Cs [14] and that for the addition of equal weights of Na and Cs to binary eutectics containing Bi as the faceting phase, the undercooling obtained in the case of the latter was higher [15]; i.e., a greater undercooling could be produced by the addition of only about one tenth of the number of atoms of caesium as compared with sodium. Thus caesium-modification of eutectic Sb–Ge was attempted and it was found that significant undercooling resulted; i.e., the addition of as little as 0.3 wt % (0.2 at %) Cs produced an undercooling of 14° C and marked modification of the eutectic structure (Fig. 6). This is further support of the chemisorption model of modification [16].

When considering the influence of chemical additions to Sb–Ge alloys, note must be taken of the fact that the major phase (Sb) will normally facet during growth and so also be affected by the chemisorbing species. Thus it might be expected that, in contrast to Al–Si, the chemically modified microstructure might differ from that produced by

1569

rapid growth without the presence of a modifying element. Support of this view emerges from a comparison of Figs. 1f, 5 and 6, where it is seen that not only do the sodium-induced changes differ from those produced by rapid growth, but that the effects of sodium differ from those of caesium for a given concentration. Following Hunt and Hurle [17], facet formation is likely to bring about only small changes in the form of the primary Sb since it is much more abundant than the germanium.

TABLE II Room temperature compressive properties of directionally solidified Sb–11 wt % Ge eutectic alloys

Growth rate (mm h^{-1})	0.2 % offset yield strength (N mm^{-2})	UCS (N mm^{-2})	% uniform contraction	Comments
2.5	590	704	1.1	
	500*	500*	0.2*	
5.4	578	675	1.1	
	566	682	1.1	
18.0	559	622	0.7	
	550	640	0.7	
	526	616	1.2	
	510*	536*	0.4*	
	149	158	0.4	Sodium modified
	70	220	4.3	
	89	236	4.1	
	94*	150*	2.5*	
	–	153	0.1	Caesium modified
	–	153	0.1	
42.0	572	711	1.3	
	598	753	1.4	
	561	661	1.4	
	534*	594*	0.9*	
54.0	83	206	4.1	Sodium modified
	101	133	1.8	
	90	133	2.0	
	101	126	1.4	
	–	181	0.15	Caesium modified
	–	234	–	
	–	164	–	
108.0	384	390	0.3	Sb primaries and
			0.1	eutectic structure
	–	305*	0.2*	
170.0	419	452	0.7	Sb primaries and
	424	436	0.3	eutectic structure
	424	436	0.3	
	–	379*	0.1*	
1330.0	397	426	0.5	Sb primaries and
	391	407	0.3	eutectic structure
	396	423	0.4	
	–	324*	0.1*	
4000.0	–	413	0.1	Sb primaries and
	392	415	0.4	eutectic structure
	414	414	0.2	
	–	331*	0.1*	

*Specimen ends lubricated with Teflon.

3.2. Compressive properties

The compressive properties for various growth conditions are summarized in Table II and Fig. 4. At the lowest growth rate the ultimate compressive strengths (UCS) of the eutectic was about 700 N mm^{-2}. Further increases in growth rates up to 42 mm h^{-1} did not produce substantial changes in the compressive properties. At a growth rate of 108 mm h^{-1}, the UCS dropped to a value of 390 N mm^{-2}. It is interesting to note that this growth rate corresponds to the appearance of the faceted Sb primaries in the microstructure. Beyond this growth velocity the UCS of the eutectic again changed little up to a rate of 4000 mm h^{-1}. Modification of the eutectic microstructure with either Na or Cs caused further decreases in the UCS values.

The fact that the presence of the Sb primaries does in fact reduce the UCS of the alloys was further substantiated by carrying out compressive tests on Sb–16% Ge hyper-eutectic alloys unidirectionally solidified at rates of 18, 54 and 1330 mm h^{-1}, Table III. The microstructure of these alloys consisted of both Ge and Sb primaries surrounded by the eutectic structure, the fineness of which increased with the growth rate. The UCS of these alloys varied between 445 and 509 N mm^{-2} and are found to be less than those of Sb– dendrite free eutectic alloys. However, the average UCS of the hyper-eutectic alloys was higher than that of the eutectic alloys containing Sb primaries. This increase may be attributed to the higher

strength germanium primaries. Sodium modification of the hyper-eutectic alloys again caused dramatic decreases in the UCS values.

It may be noted that during compression testing the eutectic used to shatter into pieces parallel to the compression axis and the pieces used to fly in all direction. This behaviour was independent of the composition and freezing rate.[‡] In order to keep the specimens for fractography, care was taken to discontinue the test just at the UCS level.

The ducitility results are equally interesting. Polycrystalline antimony is known to be brittle [18]. In the present investigation, however, some ductility was observed in the Sb–Ge alloys. The amount of ductility was found to be dependent on the eutectic morphology. Thus, the compressive fracture strain of the Sb primary–free eutectic alloys was about 1%. The presence of the Sb primaries decreased the fracture strain and in some cases the specimens used to fracture in the yield region. Caesium modification of the eutectic alloys also produced similar ductility. By contrast, Na modification caused significant increases in the uniform contraction of the eutectic alloys only.

4. Discussion

The results of the compressive tests show that the strength is virtually independent of the fineness of the eutectic microstructure. These results are not in agreement with the observations made in case of Al–Si [5] and Zn–Ge [7] alloys. From the nature of the variation of the UCS with growth rate, Sb–Ge eutectic alloys can be divided into two broad groups: (a) alloys which do not contain Sb primaries, and (b) alloys which contain Sb primaries. The average UCS of the former group is about 670 N mm^{-2} and that of the latter group is 420 N mm^{-2}. This corresponds to a decrease of about 38% in UCS, due to the presence of the Sb primaries. However, in each group the compressive strengths are essentially independent of solidification rates. This tends to indicate that the strength is controlled by flaws produced during unidirectional solidification and so is independent of the scale of the microstructure. It is presumed that such cracks form either within or around the particles of the dispersed Ge phase as a result of the development of the residual stresses following cooling from the eutectic temperature, since there is a marked difference in thermal expansion
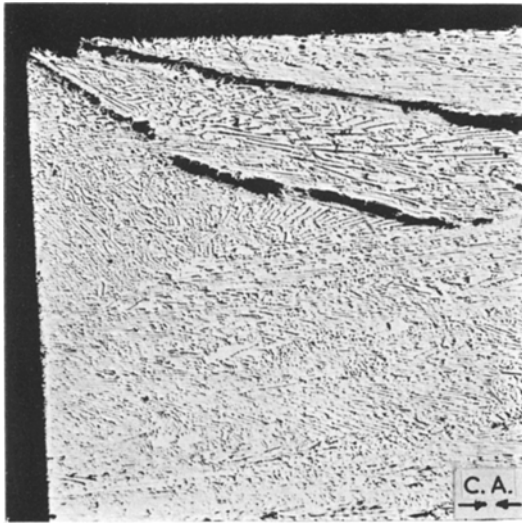
TABLE III Room temperature compressive properties of directionally solidified Sb–16% Ge hypereutectic alloys

Growth rate (mm h^{-1})	0.2 % offset yield strength (N mm^{-2})	UCS (N mm^{-2})	% uniform contraction
18	480	480	0.2
	466	466	0.2
54	482	509	0.5
	434*	472*	0.5*
	–	421*	0.1*
	–	237†	0.1†
	233	233†	0.2†
1330	–	441	0.1
	438	471	0.3
	391	445	0.5

*Specimen ends were coated with soft solder.
† Sodium modified.

‡This also occurred when the specimen ends were lubricated with Teflon or soft solder.

Figure 7 Optical micrograph of the compressive fracture surface of the hypereutectic Sb—16 wt % Ge alloy directionally solidified at 18 mm h⁻¹ (X 38). (C.A. = compressive axis).

coefficient (α) of the two phases ($\alpha_{Sb} = 8{-}11 \times 10^{-6}$ °C⁻¹ and $\alpha_{Ge} = 6 \times 10^{-6}$ °C⁻¹ [19]).

Cracks can also form during deformation due to stress concentration at the specimen—compression anvil interface and then spread along the direction of the maximum shear stress [20]. In the case of the Sb—Ge eutectic the growth direction, ⟨1 1 0⟩, is almost coincident with the direction of maximum shear stress and, as mentioned earlier, the compressed specimens would fracture parallel to the growth direction. Optical examination of the longitudinal section of the compressed specimens (Fig. 7) indicates that cracks do nucleate at the specimens—compression anvil interface and spread along the compression axis.

If the compressive strength of the eutectic is being controlled by the flaws, formed during either unidirectional solidification or deformation, the critical flaw size to initiate fracture in a brittle material can be estimated from the modified Griffith equation [21].

$$\sigma = \frac{1}{Y} \frac{\sqrt{(2E_c\gamma)}}{c} \qquad (2)$$

where

σ = fracture strength
Y = size factor ($\sim$2)
E_c = elastic modulus
γ = surface energy
c = critical flaw size, providing the various parameters are known.

The elastic modulus of the eutectic (E_c) can be estimated from the rule of mixtures

$$E_c = E_f V_f + E_m V_m \qquad (3)$$

where V is the volume fraction and subscripts f and m refer to second phase and matrix respectively. For Ge, $E_{100} = 103 \times 10^3$ N mm⁻² [22] and for Sb $E_{110} = 57 \times 10^3$ N mm⁻² [23]. Substitution of these values into Equation 3 predict a value for E_c of 62.7×10^3 N mm⁻².

If the surface energy, γ, for fracture is assumed to be the phase boundary energy between the Sb phase and the Ge phase, then γ can be calculated from λ and R measurements. According to Tiller's theory of eutectic solidification [24],

$$\gamma = \frac{A^2 L_E \rho_E \theta B (C_E - C_\alpha)}{8 T_E D \left(\dfrac{1}{m_\beta} - \dfrac{1}{m_\alpha}\right)} \qquad (4)$$

where

$A = \lambda\sqrt{R}$
θ, B = arbitrary constants (assumed equal to unity)
L_E = latent heat of fusion of eutectic liquid
ρ_E = density of eutectic liquid
C_E = eutectic composition (wt %)
C_α = composite of α phase (Sb—rich)
T_E = eutectic temperature
D = diffusion coefficient in liquid
m_α, m_β = slope of α and β liquidus lines

The following values appear suitable for the calculation of γ. $\lambda^2 R = 2.5 \times 10^{-9}$ cm³ sec⁻¹; $L_E = 46.6$ cal g⁻¹ computed from L_{Sb} and L_{Ge} [19] on a simple addition basis; $\rho_E = 6.3$ g cm⁻³ computed from ρ_{Sb} and ρ_{Ge} [19] on a simple addition basis; $C_E = 11$ wt % Ge; $C_\alpha = 1.8$ wt % Ge; $T_E = 863$ K; $m_\alpha = 4.5$° C (wt %)⁻¹; and $m_\beta = 9$° C (wt %)⁻¹. With these values, the interfacial energy γ is found to be equal to 4600 erg cm⁻². Considering the fact that the interphase boundaries represent the junction of low index planes of each phase, the interphase boundary energy estimated from Equation 4 seems to be very high. Alternatively, it is noted that preferred cleavage planes for Sb [25] are (1 1 1), (1 1 0) and (1 1 $\bar{1}$). Arguing that the plane of minimum surface energy should be the cleavage plane, and since Sb—Ge alloys tended to fracture parallel to the compressive axis, the cleavage plane can be assumed to be (1 1 0). The surface energy for (1 1 0) planes of
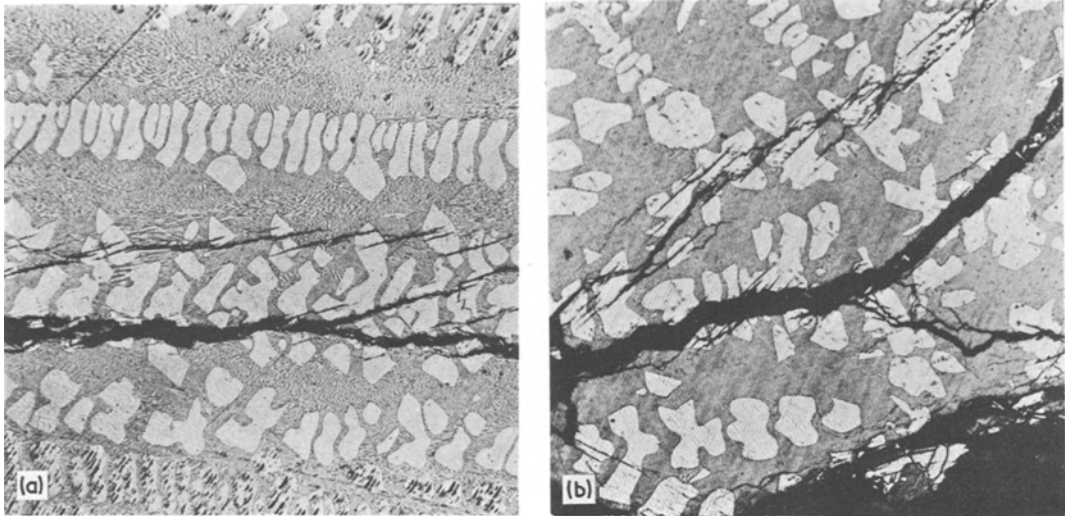
1572

Figure 8 Optical micrograph of the compressive fracture surface of the Sb–Ge eutectic directionally solidified at 4000 mm h^{-1} (× 192). (a) Longitudinal; (b) transverse.

Sb, estimated from Gilman's equation (Equation 16, [26], is 400 erg cm^{-2}. It is well known that the presence of the second phase leads to an increase in surface energy provided the particle size of the dispersed phase is significantly larger than the grain size [27]. However, in the case of Sb–Ge alloys, the grain size was found to be larger than the particle size, Fig. 1b. An equivalent value for germanium appears to be 1110 ergs cm^{-2} for fracture on {1 0 0} [26].

Thus, if we substitute in Equation 2 $\sigma = 670$ N mm^{-2}, $E_c = 62.7 \times 10^3$ N mm^{-2} and $\gamma = 4600$ erg cm^{-2}, then an upper limit for the critical crack size which would initiate fracture is estimated to be about 0.3 μm. Since the estimated crack size is very small with respect to the interparticle spacings obtained with this system, even at a freezing rate of 4000 mm h^{-1}, the strength is expected to be relatively insensitive to changes in λ. Thus the decrease in UCS due to the presence of the Sb primaries must be attributed to the ease of crack propogation in these. Evidence for this claim may be found in Figs. 8a and b which are the optical micrographs of the compressed
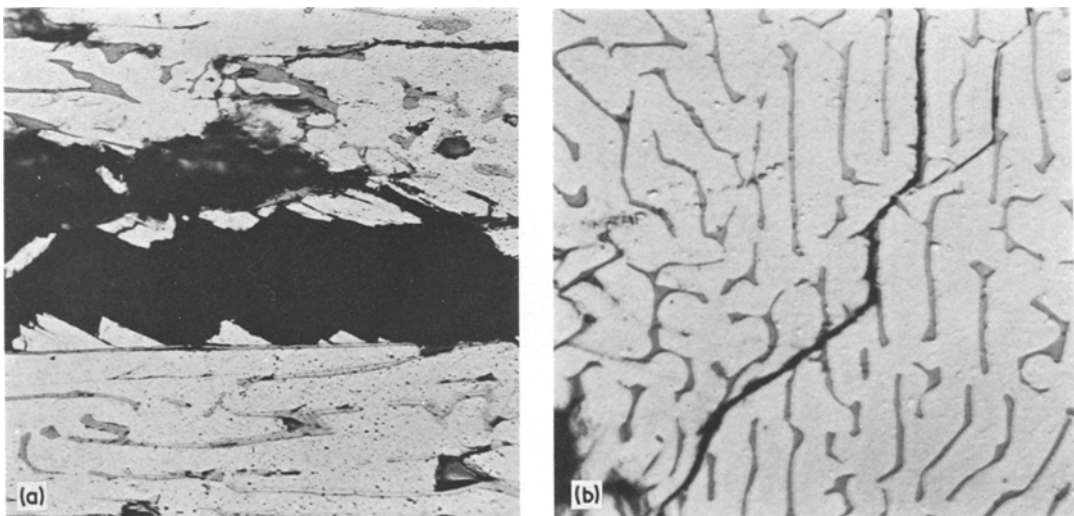

Figure 9 Optical micrograph of the compressive fracture surface of the Sb–Ge eutectic directionally solidified at 42 mm h^{-1}. (a) Longitudinal (× 480); (b) transverse (× 960).

1573

specimen unidirectionally solidified at a rate of 4000 mm h^{-1}. The figures depict crack propogation through the Sb primaries. By contrast, in alloys which do not contain Sb primaries, the cracks tend to propagate at the interface of the two phases and rarely cross the germanium phase (Figs. 9a and b). It is noted that when some of the primary antimony is replaced by germanium a slight increase in UCS occurs. This is consistent with the larger value for γ for germanium.

In comparing the mechanical behaviour of the Sb–Ge eutectic ($V_f = 12\%$) with that of both the Al–Si eutectic ($V_f = 15\%$) and Zn–Ge eutectic ($V_f = 7\%$), all structurally similar irregular eutectics, two points of divergence may be noted. The first concerns the fact that whereas the strengths of the growth- and chemically-modified Al–Si and Zn–Ge alloys were similar, the addition of Na or Cs to produce a modified structure markedly weakens Sb–Ge. Since the latter fails by cleavage and decoherence at Sb/Ge surfaces it was presumed that the chemisorbing species reduce the surface energy. To test whether the cleavage energy of the Sb itself was reduced, similar compression specimens were prepared from pure Sb and Sb–0.5 wt % Na alloys. These were then tested and it was found that the average UCS values were similar, i.e., 124 and 138 N mm^{-2} respectively. This result is not unexpected since a relatively large solute concentration in the matrix should be necessary to significantly influence cleavage energy. Thus we are led to conclude that the reduction in strength in the presence of a chemisorbing species arises from an increased ease of decoherence at Sb–Ge interfaces. Even with very small concentrations of modifier in the melt, the crystal growth process could lead to large interfacial concentrations and therefore marked surface energy reductions.

The second point of divergence is the very high UCS of the Sb–Ge eutectic as compared with that of Al–Si and of Zn–Ge. This is considered to arise because of large matrix constraints operating during the deformation of the Sb–Ge eutectic. The covalent nature of Sb would result in very little plastic deformation before fracture and so produce a very stiff composite.

5. Conclusions
(1) The Sb–Ge eutectic has been directionally solidified at rates of 2.5 to 4000 mm h^{-1}. The interparticle spacing of this irregular eutectic

decreased with increasing growth rates. The faceted Sb primaries started to appear at a freezing rate of 108 mm h^{-1}. At extremely fast growth rates the microstructure was modified to produce a fibrous form of Ge.

(2) An addition of Na or Cs to the melt also produced modification of the microstructure. However, such changes in the microstructure were different from those produced by rapid growth. In addition, for a given concentration, the changes induced by Cs were found to be better than those by Na.

(3) The UCS of the eutectic was found to be independent of the scale of the microstructure. Dramatic decreases in the UCS of the alloys were observed in the presence of the Sb primaries. The strength is thought to be controlled by the flaws created either during directional solidification or during compression testing. The presence of Sb primaries is thought to enhance the ease of crack propogation.

(4) Chemical modification of the eutectic caused further decreases in the UCS. This is attributed to decreases in Ge/Sb interface energy by the chemisorbing species.

References
1. J. D. HUNT and K. A. JACKSON, *Trans. Met. Soc. AIME* **242** (1966) 843.
2. M. N. CROKER, R. S. FIDLER and R. W. SMITH, *Proc. Roy. Soc.* **A335** (1975) 15.
3. M. N. CROKER, M. McPARLAN, D. BARAGAR and R. W. SMITH, *J. Crystal Growth* **29** (1975) 85.
4. M. N. CROKER, D. BARAGAR and R. W. SMITH, *ibid.* **30** (1975) 198.
5. M. SAHOO and R. W. SMITH, *Met. Sci.* **9** (1975) 217.
6. *Idem, Canad. Met. Quart.* **15** (1976) 1.
7. *Idem, J. Mater. Sci.* **11** (1976) 1125.
8. M. SAHOO, R. A. PORTER and R. W. SMITH, *ibid.* **11** (1976) 1680.
9. M. SAHOO and R. W. SMITH, *ibid.* **13** (1978) 283.
10. M. HANSEN and K. ANDERKO, "Constitution of Binary Alloys" (McGraw–Hill Book Co., New York, 1958).
11. R. P. ELLIOT, "Constitution of Binary Alloys", First Supplement (McGraw–Hill Book Co., New York, 1965).
12. F. A. SHUNK, "Constitution of Binary Alloys", Second Supplement (McGraw–Hill Book Co., New York, 1969).
13. H. W. KERR and W. C. WINEGARD, *Can. Met. Quart.* **6** (1967) 85.

14. V. PALM and K. PALTO, *Electrokhimiga* **9** (1971) 1312.
15. D. BARAGAR, M. SAHOO and R. W. SMITH, *J. Crystal Growth* **41** (1977) 278.
16. M. N. CROKER, Ph.D. Thesis, University of Birmingham, UK (1971).
17. J. D. HUNT and D. T. J. HURLE, *Trans. Met. Soc. AIME* **242** (1968) 1043.
18. D. P. SHASHKOV, "The Physics of Metals and Metallography", **30** (1970) 150.
19. C. J. SMITHELLS, "Metals Reference Book", Vols. I and III, (Butterworths, London, 1967) p. 225 and 685.
20. R. J. CHARLES, Proceedings of an International Conference on the Atomic Mechanisms of Fracture (John Wiley and Sons, Inc., New York, 1959) p. 225.
21. R. W. DAVIDGE and G. TAPPIN, *Proc. Brit. Ceram. Soc.* **15** (1970) 47.
22. M. E. FINE, *J. Appl. Phys.* **24** (1953) 338.
23. P. A. MAKSIMYUK and A. E. BELYAEV, *Sov. Phys. Solid State* **15** (1974) 1877.
24. W. A. TILLER, "Liquid Metals and Solidification" (American Society for Metals, Cleveland, Ohio, 1958) p. 276.
25. C. S. BARRETT and T. B. MASSALSKI, "Structure of Metals" (McGraw–Hill Book Co., New York, 1966) p. 416.
26. J. J. GILMAN, Proceedings of an International Conference on the Atomic Mechanisms of Fracture (John Wiley and Sons, Inc., New York, 1959) p. 193.
27. F. F. LANGE, "Composite Materials", Vol. 5, edited by L. J. Broutman (Academic Press, New York, 1974) p. 1.